Journal of Sound and Vibration 330 (2011) 1950–1963

Contents lists available at ScienceDirect

Journal of Sound and Vibration

journal homepage: www.elsevier.com/locate/jsvi

Characterization of elastic parameters of acoustical porous materials from beam bending vibrations

A. Renault [a,*], L. Jaouen [b], F. Sgard [c]

[a] LVA, Bâtiment St. Exupéry, 25 bis avenue Jean Capelle, F-69621 Villeurbanne Cedex, France
[b] Matelys - Acoustique and Vibrations, 20/24 rue Robert Desnos, F-69120 Vaulx-en-Velin, France
[c] IRSST 505, boulevard Maisonneuve Ouest, Montreal, Canada QC-H3A 3C2

ARTICLE INFO

Article history:
Received 18 June 2010
Received in revised form
8 November 2010
Accepted 12 November 2010
Handling Editor: I. Trendafilova
Available online 4 December 2010

ABSTRACT

Dynamic visco-elastic characterization of porous material parameters shows a revival of interest since a few years. In this article, a methodology for the assessment of the visco-elastic parameters of soft, highly damped porous materials is presented. This method uses a frequency response function of a free–free bending beam. The global method is based on an inversion procedure. It consists of fitting the experimental data to the GLM computation model. In the experimental part of this work, it is explained how to take the attachment system and sensor mass into account and how to measure it. The assessment of the visco-elastic parameters needs a discrete laminae analytic model. The GLM model is described and used for a sensitivity study in relation to the visco-elastic parameters. This study gives indications for the beam dimensions design. The results, bending modulus and loss factor in the beam's main direction for various frequencies, obtained for two polymeric foams are shown and compared to results obtained with other techniques. The originality can be found in the experimental developments but also on technical developments of parameters assessment.

1. Introduction

Industry needs characterization of porous materials because their dynamic visco-elastic parameters serve as input data for modelling. Moreover, new materials are developed and it is necessary to know their properties in order to link for example their chemical composition to their mechanical characteristics. For the assessment of dynamic visco-elastic parameters, several methods exist. The Oberst method [1], based on clamped–free beams, can be applied to visco-elastic materials such as dense polymers. The identification procedure is defined by the ASTM-E756-98 [2] standard. A method developed by Wojtowicki et al. [3], inspired by the Oberst method, has been proposed in 2004. It is based on transfer function measurement and computation of a free–free beam excited at its center. The drawbacks of the latter method are that the fixation at the beam center is not easily controlled and the computation can be time consuming if finite elements are used for numerical simulation (in case of thick materials for example). Recently, in [4], Liao et al. also proposed a modified Oberst method for complex Young's modulus assessment. Continuous frequency dependant Young's modulus of a soft polymer is calculated in combining measured transfer functions along the beam and wave coefficient computations. Even if the tested material are soft, they are not as light as porous foams. Beam-shaped samples are usually employed for the assessment of porous material visco-elastic parameters because of their simplicity. However, in [5], plate samples have been used. The samples have to be

* Corresponding author.
E-mail addresses: arenault81@gmail.com, amelie.renault@insa-lyon.fr (A. Renault).

0022-460X/$ - see front matter © 2010 Elsevier Ltd. All rights reserved.
doi:10.1016/j.jsv.2010.11.013

large and the computation is more time consuming. In order to get the parameters at higher frequencies, acoustical methods have been developed and are described in [6–8]. These methods apply to porous material saturated with air. They require that the frame compressional Biot wave velocity and either shear Biot wave velocity or Rayleigh wave velocity are measured and simulated. For frame compressional Biot wave measurement, a sample is placed in a rigid backing and is excited with a monopole. The displacement is measured with a laser doppler vibrometer. For experimental Rayleigh wave velocity measurement, the porous material sample is placed in a rigid backing too. A magnetic transducer is used in order to excite Rayleigh waves within the material. The advantages and drawbacks of the different methods allowing an estimation of visco-elastic parameters of porous materials is summarized in Ref. [9], by comparing results for a Melamine foam.

In this article, the focus is on methods based on bending vibrations of a multi-layer beam excited mechanically. The beam is composed of a base beam onto which the tested porous layer is bounded. Providing that the visco-elastic properties of the base beam are known, the comparison of measured and calculated frequency response functions (FRF) allows to obtain the properties of the tested material: its frequency dependent Young's modulus and structural damping. The frequency range under study is 10–2000 Hz. Compared to [3,4], the set-up is simplified: the used FRF is the input mobility, which is simpler to measure than the transfer mobility, using a single impedance head. The boundary conditions are also better controlled. A novel way of analytical modelling has been developed in order to considerably reduced the computation time.

In the first section, the methodology of the present approach is described. In the second part, equations used for the analytical simulation of the system are presented. The fitting between modelled and measured FRF is done using resonant frequencies, easily identifiable from experimental FRF data. The experimental layout has to be sensitive to variations in material parameters, which means that for a given parameter variation, the FRF variation should be significant. A function quantifying the parameter dependence on resonance peaks is thus defined and calculated for several beam dimensions. The third section is dedicated to experimental studies. The set-up and procedures are explained in details. The evaluation of the base beam visco-elastic parameters is described in the fourth part. In fact, the accuracy of the method depends a lot on these parameters. The last part shows the application of the inversion method used to several porous materials, all of which is followed by the conclusion.

2. Methodology

This section gives a layout about the methodology under study for porous material mechanical parameters assessment. The latter uses as FRF the input mobility defined as

$$\tilde{\mathrm{FRF}} = \frac{\tilde{W}}{\tilde{F}} \tag{1}$$

$\tilde{F}$ is the injected force complex amplitude in Newton, $\tilde{W}$ the velocity in m/s at the excitation point.

Fig. 1 shows a schematic description of the methodology. The different steps to be done in order to extract the visco-elastic properties of porous material are:

1. FRF measurement.
2. FRF modelling using an appropriate model.

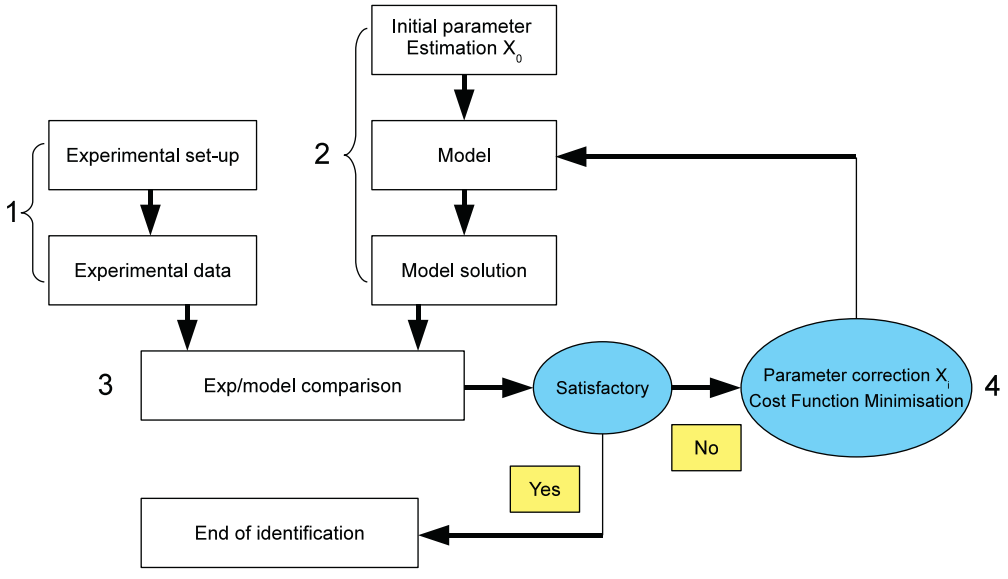

Fig. 1. Scheme of the methodology. X is the parameter to be identified.

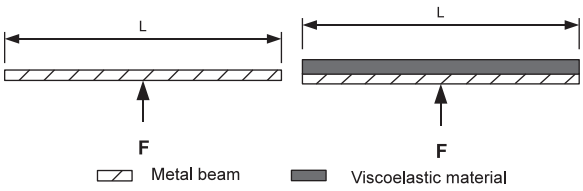

Fig. 2. Beam configurations.

3. Cost function definition (quantification of the measured and calculated FRF difference).
4. Cost function optimization for the assessment of parameters.

Two different layouts are used, as shown in Fig. 2. The vibratory response of the base beam, which is assumed to be homogeneous, is calculated using a modal approach. Regarding the two-layered beam, a discrete layered model is used to predict the FRF. A brief description of the latter is done next.

3. Sensitivity study of a multi-layer beam

The optimization process requires repetitive computations, which in return, demands for a time-efficient computation algorithm. Shortening the computation time will allow not only an increasing efficiency of test procedure but also the optimization of the experimental set-up. The latter will be done by a parameter study.

3.1. Discrete-layer model

For the vibration response calculation of a multi-layer beam system, the hypothesis is done that the effect of fluid phase on the vibration of the system can be neglected. This hypothesis is valid since the samples respect the criteria that the volume over the lateral surface area is lower than 0.02 (see the conclusions of the study done in [10]). An analytical code calculating the multi-layer beam's response, in which a Mindlin displacement type in each layer is assumed, has been developed by Ghinet and Atalla [11,12]. Assuming a transverse displacement $W = A_1\cos(k_c x_1)+B_1\sin(k_c x_1)+A_2\cosh(k_c x_1)+B_2\sinh(k_c x_1)$ and using the appropriate boundary conditions, the input mobility writes

$$\tilde{\mathrm{FRF}}_c = \frac{\tilde{\tilde{W}}(x_1 = L/2)}{\tilde{F}(x_1 = L/2)} = \frac{\mathrm{j}\omega\left(1+\cosh\left(\frac{k_c L}{2}\right)\cos\left(\frac{k_c L}{2}\right)\right)}{\left(\cosh\left(\frac{k_c L}{2}\right)\sin\left(\frac{k_c L}{2}\right)+\sinh\left(\frac{k_c L}{2}\right)\cos\left(\frac{k_c L}{2}\right)\right)k_c^3\{EI\}_{\mathrm{eq}}} \tag{2}$$

k_c being the first propagative wavenumber of the layered system. This wavenumber is the solution of the dispersion equation in terms of an unknown vector containing displacement and force components (it is obtained in Refs. [11,12]). The relation between $\{EI\}_{\mathrm{eq}}$ and k_c is

$$\{EI\}_{\mathrm{eq}} = \frac{\omega^2\rho}{k_c^4} \tag{3}$$

where E is Young's modulus of the layered system, I the area moment of inertia about the neutral axis, ω the angular velocity and ρ the equivalent density of the multi-layer. The material in each layer is supposed to be isotropic and homogeneous.

3.2. Sensitivity study

This part treats a metal–porous material bi-layered beam. FRF resonances correspond to flexural modes. Fig. 3 shows the first five flexural mode shapes symmetrical with respect to beam's center, for a free–free beam layout. The illustrations have been carried out with the help of FEMAP, the modes shape being computed under Nastran.

In order to evaluate the difference between experimental and simulated FRF, a particular cost function will be defined. It is the relative difference between the k-th resonant frequency $\omega_{0,k}$ and ω_k^i obtained respectively from the experimental and simulated FRF at the i-th iteration:

$$\mathrm{CF} = \left|\frac{\omega_k^i-\omega_{0,k}}{\omega_{0,k}}\right| \tag{4}$$

This cost function can be numerically calculated for two values of an input parameter. If p_j is a parameter taking the values p_j^i and p_j^{i+1} at the i-th and $(i+1)$-th iteration respectively, in linear approximation, the cost function writes

$$\mathrm{CF}(p_j^{i+1}) = \mathrm{CF}(p_j^i)+\mathrm{CF}'(p_j^i)(p_j^{i+1}-p_j^i) \tag{5}$$

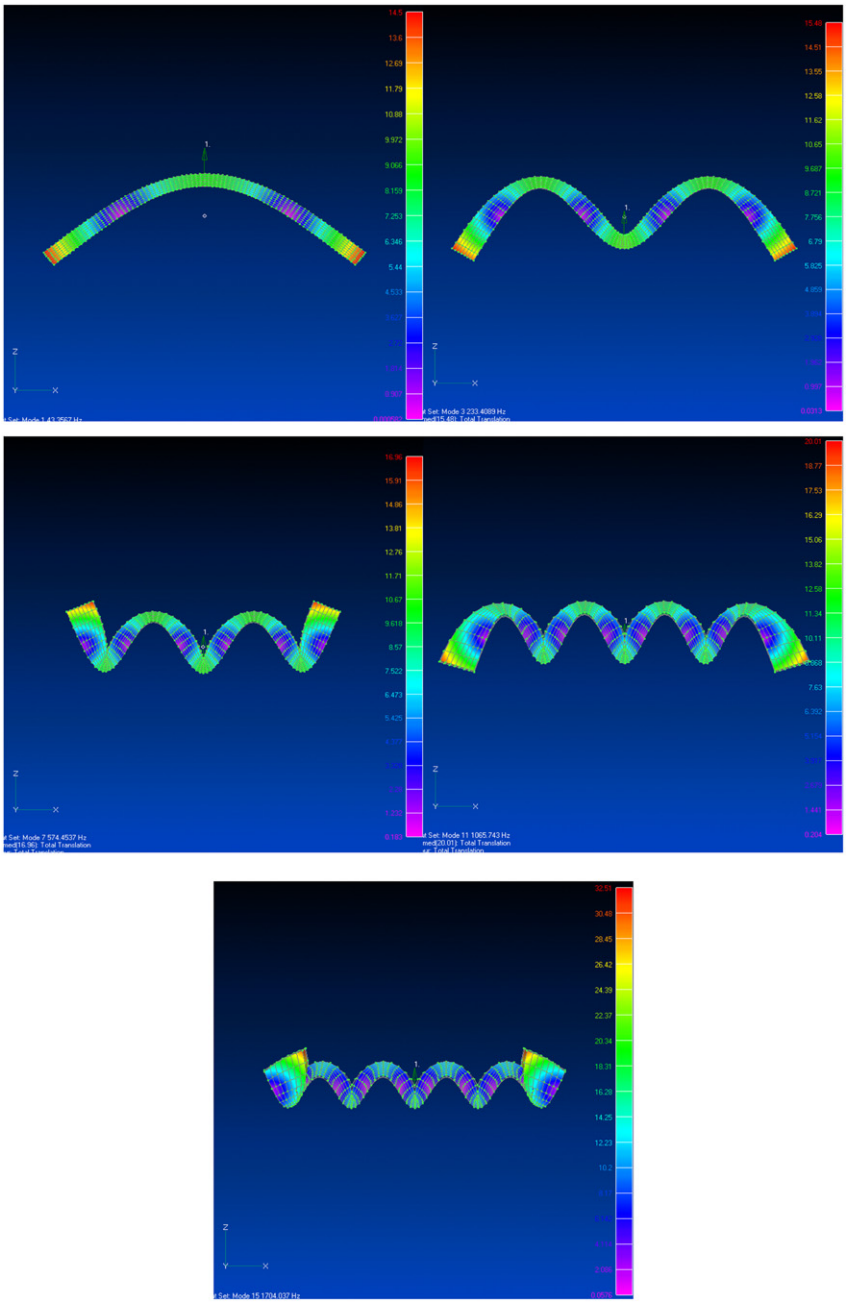

Fig. 3. First five symmetric mode shapes of the bi-layered beam.

where CF′ denotes the first derivative of CF. The theoretical first derivative of the cost function given in Eq. (5) quantifies the model sensitivity to the variation of the imposed parameter p_j. For the j-th mode and the i-th iteration, a sensitivity function S can be defined as

$$S(\alpha) = \left| \frac{(\omega_j^{i+1} - \omega_j^i)}{(\alpha - 1)} \frac{1}{\omega_j^i} \right| \times 100 \tag{6}$$

The sensitivity is defined as a function of the relative variation of parameter, $\alpha = p_j^{i+1}/p_j^i$, because the order of magnitude of the parameters under study is extremely different (about 10^6 for Young's modulus and 10^1 for Poisson's ratio). In the following, the sensitivity function is studied in the case of bi-layered beam 'metal–porous material'. For different beam

geometries (see Table 1 for details), ω_j^i and ω_j^{i+1} are assessed from the simulated FRF for two parameter values such that $\alpha = 1.1$. This relative variation has been chosen in order to give realistic increment steps, neither too large nor too small.

Fig. 4 shows two examples of the evolution of the function S as a function of the mode index j. The beam length is fixed at 0.3 m and the base beam thickness at 0.01 m. The thickness of the porous material is 0.01 m for the case (a) and 0.025 m for the case (b). One can notice that the sensitivity is globally decreasing with the mode index. The modes higher than the tenth show too low sensitivity for the correct assessment of Young's modulus of the porous layer. The larger the porous material thickness, the larger the sensitivity.

The conclusion of the study, described in [13], is that it is possible to determine Young's modulus in the bi-layered configuration because the model is sensitive enough to this parameter. Concerning Poisson's ratio, it is shown that the sensitivity is much lower for this parameter than the one calculated for Young's modulus. With this technique, Poisson's ratio identification cannot be accurate enough.

In order to get the best sensitivity, the following rules are recommended:

- a thin base beam compared to the porous material thickness to be tested;
- a base beam stiffness being as close as possible to that of the tested material;
- a beam length of about 0.3 m.

Those conclusions are coherent with the one given in [4] where it is specified that the thickness ratio between the layer and base beam should be high for the uncertainty to be low.

The above study is done for a known structural damping. In real case, the damping has to be identified too. As the identification of the damping can be difficult using the -3 dB bandwidth method, it can be done simultaneously with the identification of Young's modulus. For that purpose, it is necessary to define a new cost function based on the FRF. The relative differences between measured and calculated FRF are summed for discrete frequencies around the resonance frequency of interest, which gives the following cost function:

$$\mathrm{CF}_{\mathrm{FRF}} = \sum_n \frac{|\tilde{Y}_{\mathrm{mes}}(\omega_i) - \tilde{Y}_{\mathrm{calc}}(\omega_i)|}{|\tilde{Y}_{\mathrm{mes}}(\omega_i)|} \tag{7}$$

$\tilde{Y}_{\mathrm{mes}}$ is the measured FRF and $\tilde{Y}_{\mathrm{calc}}$ is the computed one. n is the number of frequency points.

The next section is dedicated to the FRF measurements.

Table 1
Beam configurations used for the sensitivity study. ρ is the material density, E is Young's modulus, η the structural damping, and ν the Poisson's ratio.

	ρ (kg m^{-3})	E (N m^{-2})	ν (–)	η (–)	Length (mm)	Thickness (mm)
Base beam	6249	9.7×10^{10}	0.33	0.01	200 300 400	1 1.5 2
Porous material	9	120 000–132 000	0.33–0.37	0.1	200 300 400	10 25

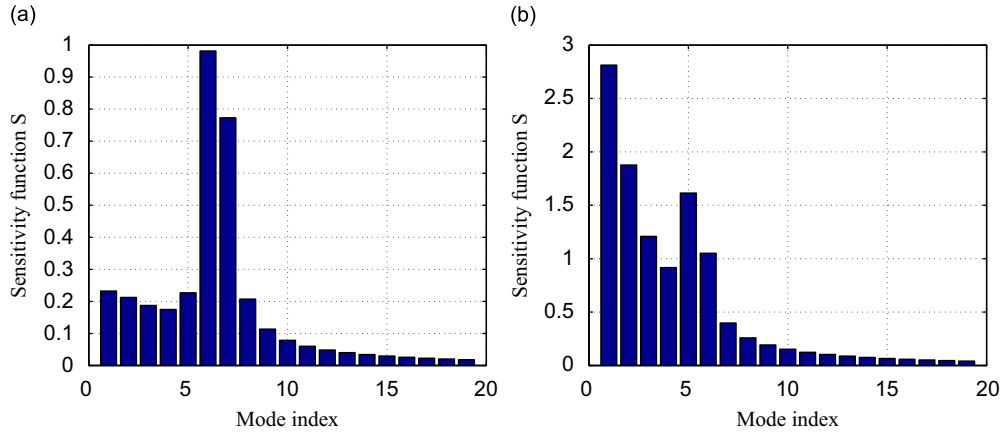

Fig. 4. Influence of porous material thickness on Young's modulus sensitivity, for a given Poisson's ratio $\nu = 0.35$. (a) $D_b/D_p = 970$, (b) $D_b/D_p = 62$. D_b is the base beam bending stiffness and D_p is the bending stiffness of the porous material.

Fig. 5. Experimental set-up.

4. Experimental studies

4.1. Description of the experimental set-up

The experimental set-up consists of a beam in the center of which a screw is glued. The beam is connected to the shaker with this screw (cf. Fig. 5). The input mobility is measured at the beam center, the beam having free–free boundary conditions. The driving force and acceleration are measured with a PCB 288D01 impedance head. The acquisition card, a soft dB Signal Ranger one, is linked to a computer via a USB cable. The shaker, a BK 4809 type, is connected to an amplifier. The excitation is a pseudo-random noise. The frequency resolution is 0.25 Hz. It has been found that the measurements were repeatable with high accuracy. The reproducibility is good enough so that it does not influence the determination of the visco-elastic parameters of the base beam and porous materials (see Section 5 for more details). In fact, the mode resonance frequency can be found with an incertitude of only a few Hz.

4.2. Impedance head and screw mass effect

The force which excites the beam is not the one measured by the impedance head because of the mass of the attachment system and the residual mass of the impedance head. If m_0 denotes the corresponding total added point mass, the corrected input mobility $\tilde{Y}_{\mathrm{mc}}$ reads [14,15]

$$\tilde{Y}_{\mathrm{mc}} = \frac{\tilde{\tilde{W}}_{\mathrm{mes}}}{\tilde{F}_{\mathrm{mc}}} = \frac{\tilde{\tilde{W}}_{\mathrm{mes}}}{\tilde{F}_{\mathrm{mes}} - m_0 \tilde{\tilde{W}}_{\mathrm{mes}}} = \frac{\tilde{Y}_{\mathrm{mes}}}{1 - \mathrm{j}\omega m_0 \tilde{Y}_{\mathrm{mes}}} \tag{8}$$

$\tilde{\tilde{W}}_{\mathrm{mes}}$ and $\tilde{\tilde{W}}_{\mathrm{mes}}$ are the measured acceleration and associated velocity respectively, $\tilde{Y}_{\mathrm{mes}}$ is the measured input mobility.

Considering the impedance head in free state, the modulus of apparent mass $|\tilde{F}_{\mathrm{mes}}/\tilde{\tilde{W}}_{\mathrm{mes}}|$ corresponds to m_0. Fig. 6 shows the variation of this ratio, for the uncharged impedance head. The mean value is 0.0059 N s^2 m^{-1} (cf. Fig. 6), which implies an impedance head seismic mass of 5.9 g. If the mass of the screw is accounted for, one finds m_0=7 g. The system is shown in Fig. 7. The damping induced by the impedance head and screw mass is neglected.

The measured signal can be corrected easily using Eq. (8). But the corrected measured signal is not smooth enough. It is shown in the next part how to modify the model in order to include this point mass m_0.

4.3. Double tape effect

Fixing the double sided tape on the base beam produces an effect on vibration which is not negligible. Fig. 8 shows the comparison between the FRF of an aluminium beam with and without the tape added across the whole beam. It is seen that the tape modifies the FRF via its mass and damping. In fact, both the modal frequencies and resonance peaks are lowered. It is mentioned in [3] that the identification of visco-elastic properties of the equivalent beam+tape system should be done as a first step for accurate assessment of visco-elastic parameters of dense polymer. The measured and computed frequency response function are well superimposed when double tape weight and thickness respectively are taken into account. Given the densities of the tested materials here, this step is even more critical and is explained in detailed in the next section.

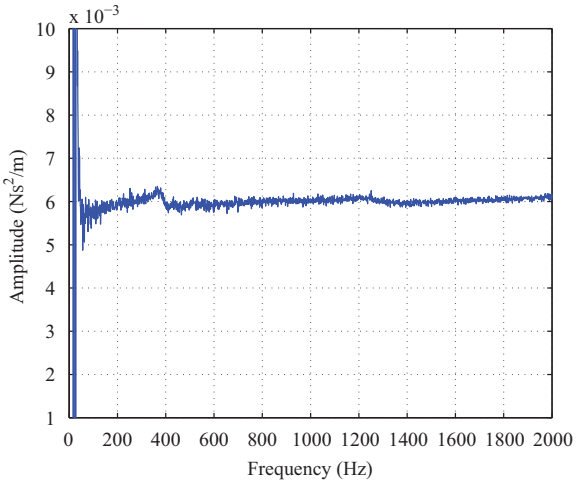

Fig. 6. Input mobility modulus of the uncharged impedance head.

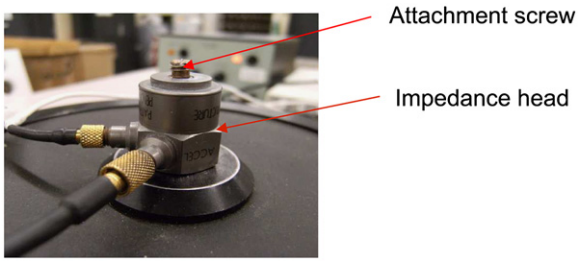

Fig. 7. Zoom on the impedance head with the screw.

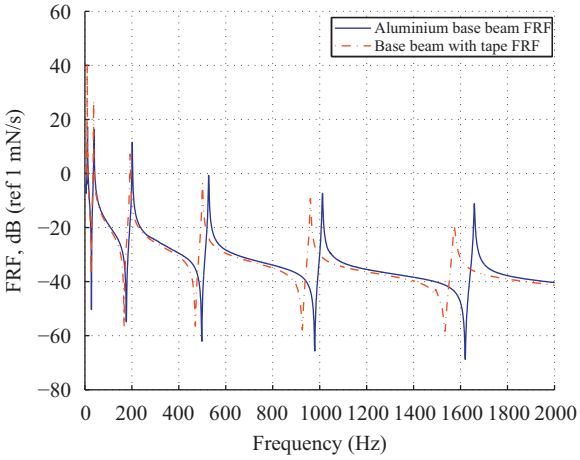

Fig. 8. Effect of double sided tape on the input mobility.

5. Examples of identification

5.1. Identification of equivalent base beam properties

5.1.1. Model description, mass correction

In this section, a finite element model is used in order to get the FRF of a homogeneous beam. The model is constructed with trigonometric shape functions [16]. As previously mentioned, a modification is done in order to add a point mass within the model. The configuration is the one shown in Fig. 9.

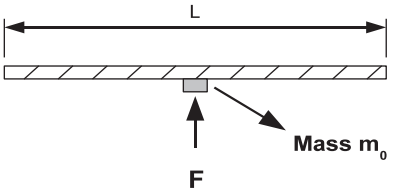

Fig. 9. Scheme of the base beam with the point mass.

Let x be the excitation position and L the beam length. A non-dimensional variable $\xi = 2/Lx - 1$ is introduced. The transverse displacement of the beam can be expressed in terms of trigonometric basis functions ϕ_m as

$$w(\xi,\omega) = \sum_n q_n(\omega)\phi_m(\xi) \tag{9}$$

for $-1 \le \xi \le 1$.

The basis functions are defined as: $\phi_m(\xi) = \sin(a_m\xi + b_m)\sin(c_m\xi + d_m)$ (see [16], where the coefficients a_m, b_m, c_m, d_m are given). Using Galerkin's approach, the current modal amplitudes $q_n(\omega)$ are the solution of the following linear system:

$$([\mathbf{K}] - \omega^2[\mathbf{M}])\mathbf{q} = \mathbf{F} \tag{10}$$

where $\mathbf{F}$ is the input force, $[\mathbf{K}]$ and $[\mathbf{M}]$ are the stiffness and mass matrices given by

$$K(m,n) = \frac{4DbI_2(m,n)}{L^3} \tag{11}$$

$$M(m,n) = Lm_s\frac{I_0(m,n)}{4} + M_0(m,n) \tag{12}$$

$$M_0(m,n) = \frac{m_0\phi_m(\xi)\phi_n(\xi)}{2} \tag{13}$$

$D = (E(1+i\eta)h^3)/12$ is the flexural stiffness of the beam, $m_s = \rho hb$ is the mass per unit length, ρ is the density, b and h denote the beam width and thickness respectively. The integrals I_0 and I_2 are defined as

$$I_0(m,n) = \int_{-1}^{1} \phi_m(\xi)\phi_n(\xi)\, d\xi \tag{14}$$

$$I_2(m,n) = \int_{-1}^{1} \frac{d^2\phi_m(\xi)}{d\xi^2}\frac{d^2\phi_n(\xi)}{d\xi^2} d\xi \tag{15}$$

In order to gain precision, it is necessary to use the measured frequency variation of the total mass m_0. Since $[\mathbf{M}_0]$ is frequency dependent, $[\mathbf{M}]$ is frequency dependent too. System (10) can be solved by finding the eigenmodes of the associated homogeneous system and then projecting the forced system onto these eigenmodes. The transverse displacement of the beam can be expressed in terms of trigonometric basis functions ϕ_n as

$$\mathrm{FRF}(\omega) = \frac{\sum_{n=1}^{N} \mathrm{j}\omega q_n(\omega)\phi_n(0)}{F_z} \tag{16}$$

5.1.2. Identification

Once the total mass of the transducer together with the fixation system included in the model, the equivalent base beam properties can be calculated. The goal is to identify the frequency evolution of Young's modulus and structural damping of the base beam with the double sided tape. The tape mass is taken into account in the equivalent beam density, which is calculated for the beam+tape system. The index bbt is used to denote this system. The equivalent base beam has the following parameters: L=0.3048 m, l=0.0255 m, $h_{\mathrm{bbt}} = 0.00115$ m and $\rho_{\mathrm{bbt}} = 2130$ kg m^{-3}. h_{bbt} is the total thickness of the beam+tape system, and ρ_{bbt} is the mass over the volume of this system. Poisson's ratio is fixed to 0.33. The tape thickness is about $h_{\mathrm{t}} = 0.0005$ m, which means that it is not negligible.

A preliminary calculation is done with RKU formula, for an aluminium beam having Young's modulus of 7.3×10^{10} Pa. The formula linking the beam+tape system Young's modulus, E_{bbt}, to the aluminium beam Young's modulus, E_{alu}, writes as follows (cf. [1]):

$$\frac{E_{\mathrm{bbt}}I_{\mathrm{bbt}}}{E_{\mathrm{alu}}I_{\mathrm{alu}}} = 1 + e_r h_r^3 + 3(1+h_r)^2\frac{e_r h_r}{1+e_r h_r} \tag{17}$$

$e_r = E_{\mathrm{bbt}}/E_{\mathrm{alu}}$ and $h_r = H_{\mathrm{bbt}}/H_{\mathrm{alu}}$, H_{bbt} and H_{alu} are the respective thickness of the base beam system and the aluminium beam. I_{bbt} and I_{alu} are the second moment of area of beam cross section corresponding to the equivalent base beam and aluminium beam

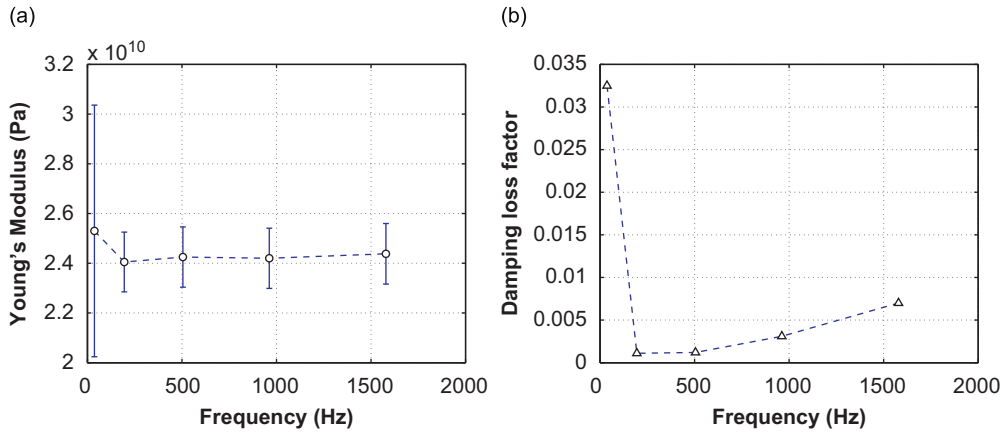

Fig. 10. Equivalent base beam properties (aluminium with double sided tape). (a) Young's modulus. (b) Damping loss factor.

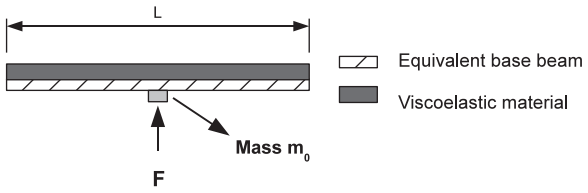

Fig. 11. Scheme of the bi-layer beam with the point mass.

respectively. Since Young's modulus of the tape is very low compared to the aluminium one, E_{bbt} can be approximated to

$$E_{\mathrm{bbt}} = \frac{E_{\mathrm{alu}} I_{\mathrm{alu}}}{I_{\mathrm{bbt}}} = E_{\mathrm{alu}} h_r^2 \tag{18}$$

The equivalent Young's modulus is found to be 2.36×10^{10} Pa. This value is used as the initial value for the optimization. Young's modulus is the result of the cost function minimization, where it is used as the optimization parameter. The equivalent density and thickness have been used. The optimization, i.e. minimization of the cost function using Eq. (5), is done in the interval $[1\text{–}5] \times 10^{10}$ Pa, with the help of the Matlab© function *fmincon*. The optimization produces identical solutions when different initial values are used: a global minimum exists in this interval. The structural damping is calculated with the -3 dB bandwidth technique at each resonance frequency. An error of 5 Hz on the resonance frequency only induces a 5 percent error on the base beam Young's modulus. Young's modulus identification error is however higher at the first resonant mode (cf. error bars in Fig. 10). This mode is in fact more sensitive to boundary conditions and Young's modulus. As said before, resonance frequency can be well determined and finally visco-elastic parameters of the base beam with double tape can be found with less than few percent error.

Fig. 10 shows the equivalent beam visco-elastic properties as a function of frequency. The evolutions of these properties with frequency are typical for a visco-elastic material.

5.2. *Identification of porous material visco-elastic properties: bi-layer beam case*

5.2.1. *Proposed approach*

In order to take into account impedance head seismic mass and screw mass, in the bi-layer beam configuration (see the layout in Fig. 11), several steps have to be followed (cf Fig. 12). First, the theoretical resonance frequencies of the antisymmetrical modes, ω_n, without added mass are calculated for the bi-layered beam with the GLM analytical code. In a second step, an equivalent Young's modulus, denoted as E_{eq}, is calculated as

$$E_{\mathrm{eq}} = \frac{\omega_n^2 \rho_{\mathrm{eq}}}{k_n^4} \frac{12}{h_{\mathrm{eq}}^2} \tag{19}$$

h_{eq} and ρ_{eq} are respectively the equivalent thickness and density of the system base beam + tape + porous material. Finally, one can treat the system as a homogeneous one and accounting for the impedance head mass is done as described previously.

The cost function used here is the one described in Eq. (7), $\tilde{Y}_{\mathrm{calc}}$ being the calculated input mobility accounting for m_0. For a good optimization, the calculated transfer function is interpolated with a 0.1 Hz step within the interval $[f_{\mathrm{res}} - 10\ \mathrm{Hz}; f_{\mathrm{res}} + 10\ \mathrm{Hz}]$, where f_{res} is the resonance frequency of the mode under study. This interval is of great importance,

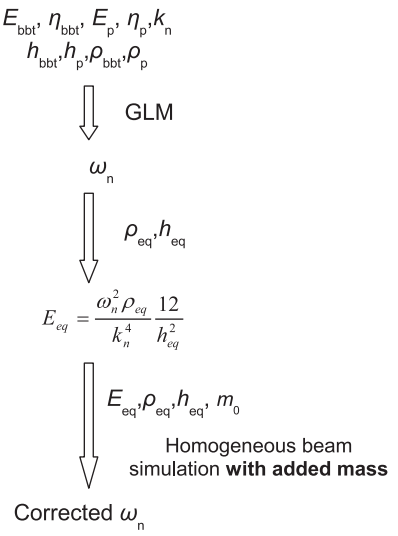

Fig. 12. Mass correction procedure. h_p, ρ_p, E_p and η_p are the porous material thickness, density, Young's modulus and damping respectively, h_{bbt}, ρ_{bbt}, E_{bbt} and η_{bbt} are the same quantities for the equivalent base beam.

Table 2
Quasistatic parameters for the foam M1. E: Young's modulus, η: structural damping factor v: Poisson's ratio. Standard deviation calculated for three tested samples

	E (N m^{-2})	η (–)	v (–)
Mean value	132 400	0.08	0.33
Standard deviation	(12 100)	(0.01)	(0.03)

since if it is too short, the cost function variation will be too small. The beam dimensions ensure that there are at least 20 Hz between two resonant modes, because there are only up to five modes in the interval [10–2000] Hz.

5.2.2. Results

Several polymeric foams having different densities have been tested and their visco-elastic properties identified. The aluminium base beam together with the double sided tape have the visco-elastic properties found in the previous section (see Fig. 10). The procedure described in the beginning of the section is used to assess Young's modulus and damping loss factor of the porous material. Poisson's ratio is set to its quasistatic value.

The visco-elastic properties of the base beam and porous material are simulated with a frequency dependence: the properties found at the resonance frequencies are interpolated on the entire frequency range. All the measurements have been made at a temperature of 23 °C.

Melamine case: In this section, a Melamine foam (M1) having a density of 8.73 kg m^{-3} and a thickness of 0.0194 m is tested. The quasistatic properties evaluated with a quasistatic method [17] are listed in Table 2. The ratio of equivalent base beam stiffness to Melamine stiffness is about 40.

The Melamine Young's modulus and structural damping visco-elastic properties, found using the proposed approach, are shown in Figs. 13 and 14. The quasistatic properties together with the properties obtained with the resonant method, cf. [17,18] respectively, are also shown. The values obtained with the different methods match well. The first mode is sensible to the boundary conditions and can be neglected. The value found for the fourth mode is low and might be underestimated. In fact, the related structural damping seems overestimated. Jaouen in [19] finds Young's modulus variation of 80 000 Pa in one decade for a Melamine foam. In the present study, the variation amplitude of this parameter is 120 000 Pa in two decades which corresponds to the same order of magnitude. Concerning the damping, Jaouen finds a maximum value at 1000 Hz at a temperature of 20 °C for the same type of Melamine. A similar evolution is found in Fig. 14 where damping is increasing up to about 1000 Hz.

The measured and calculated FRF of the bi-layered beam can be seen in Fig. 15. The curves are superimposed in a satisfying manner indicating that the identification of parameters is accurate.

Polyurethane foam case: In this section, a foam (Material M2) having a density of 5.19 kg m^{-3} and a thickness of 0.0242 m is tested. The quasistatic properties evaluated with a quasistatic method [17] are listed in Table 3. The ratio of the equivalent base beam stiffness to polyurethane stiffness is about 270.

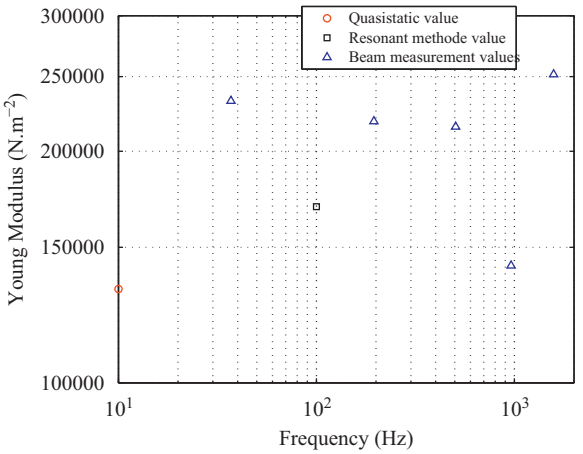

Fig. 13. Young's modulus as a function of frequency—material M1.

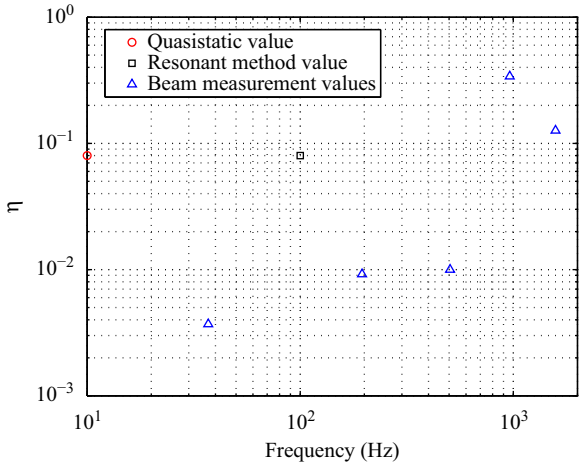

Fig. 14. Loss factor as a function of frequency—material M1.

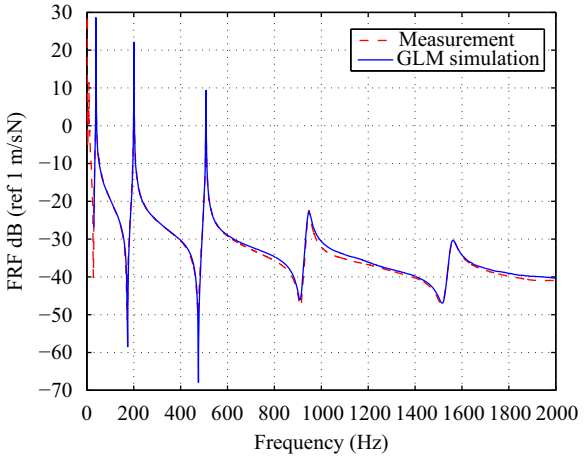

Fig. 15. Validation: simulation and measurement of the bi-layered beam (aluminium+M1).

Table 3
Quasistatic parameters for the foam M2. E: Young's modulus, η: structural damping factor ν: Poisson's ratio. Standard deviation calculated for three tested samples

	E (N m^{-2})	η (–)	ν (–)
Mean value	10 040	0.0124	0.2403
Standard deviation	(2800)	(0.0075)	(0.0027)

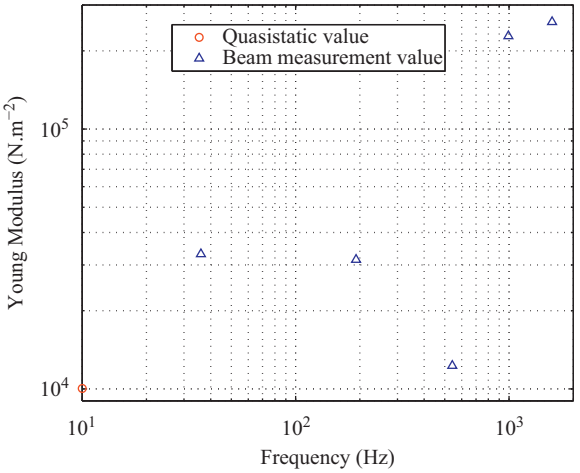

Fig. 16. Young's modulus as a function of frequency—material M2.

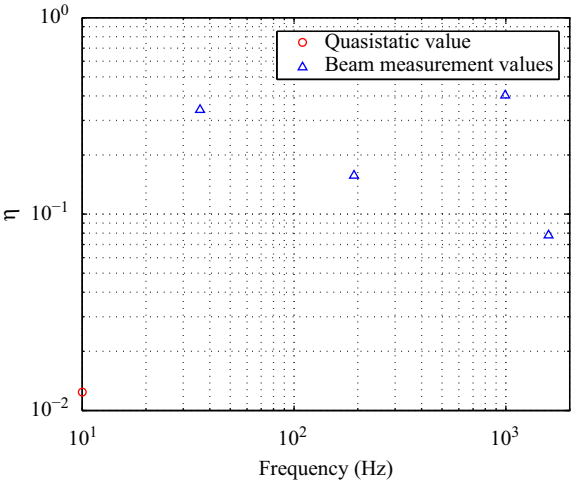

Fig. 17. Structural damping as a function of frequency—material M2.

The obtained polyurethane Young's modulus and structural damping are shown in Figs. 16 and 17. The quasistatic properties are also shown. Here, Young's modulus value found at the third mode is underestimated. Among other things, this may be due to the imperfect shape of the polyurethane beam which was difficult to cut. This influences the FRF, near the third resonance peak. This is not taken into account by the model and Young's modulus might be badly estimated. Moreover, the optimization process hardly converges. The identification problem have not been encountered in Melamine case. There might be an influence of Melamine beam cutting on the FRF but in our case, it does not occur near resonance frequencies. The irregular Young's modulus evolution with frequency shows the difficulty to measure the properties of such a light weight material.

As it has been seen in the sensitivity study, the base beam should have been thinner in order to reduce the equivalent base beam to porous material stiffness ratio. But at too low base beam stiffness the beam is statically bending under the material weight. Using a material alternative to metal, such as plexiglass, could lead to a decrease in stiffness but would nevertheless

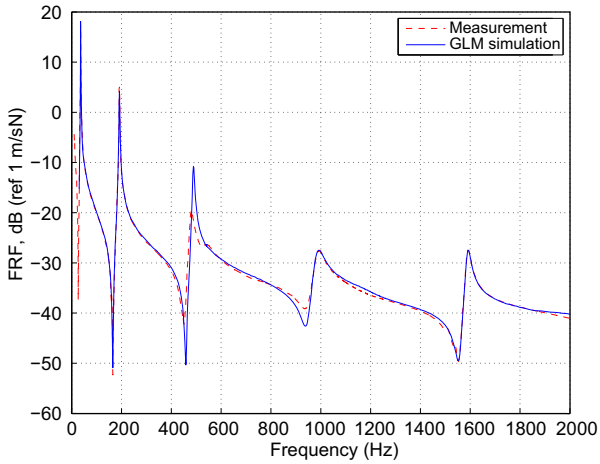

Fig. 18. Validation: simulation and measurement of the bi-layered beam (aluminium+M2).

push the resonant frequencies up, thus leading to a fewer resonant modes in the [10, 2000] Hz frequency range. Moreover, the base beam structural damping would then have been too high and more frequency dependent than aluminium. It would be difficult to precisely locate experimental resonance frequencies. The measured and calculated FRF of the bi-layered beam can be seen in Fig. 18. Here again, the two curves are anyway superimposed in a satisfying manner. The conclusion is that the parameter estimation is satisfying, except for the third mode.

6. Conclusion

The paper presents a method for dynamic measurement of Young's modulus and structural damping of visco-elastic porous materials. The described methodology is based on the comparison of measured and calculated input mobility of a free–free bi-layered beam. Foremost any test, the dynamic mass of the system screw-impedance head has to be measured. Then, frequency dependant Young's modulus and structural damping of the beam in which the tested porous material is bounded, have to be determined independently. Those properties have to be interpolated and used as input parameter for the porous material properties identification. Finally, the cost function optimization based on the resonance frequencies of the aluminium beam+tape+porous material FRF, gives Young's modulus and structural damping of the porous material under test as a function of frequency. It is possible to get values for frequencies up to 2000 Hz. For higher frequencies, the model sensitivity becomes too low to be exploitable. The results show that the recommended length for the aluminium beam should be about 0.3 m. The beam thickness has to be selected depending on the tested quasistatic material properties. The advantages of this methodology are that the experimental set-up is simple and that the impedance head measurement gives reliable results. In addition, the time needed for an inversion is very reasonable: it takes a few minutes on a desktop computer because the model used is an analytical one. The present approach leads to parameters of the same order of magnitude as the quasistatic method. The drawback is that it is sensitive to the beam geometry especially when low stiffness materials are measured.

In order to get this study completed, it could be interesting to measure the input mobility of the system at different temperatures. The frequency range could then be enhanced in using frequency-temperature equivalence, with precautions. For studies of anisotropy, similar measurements and simulations on samples cut in other directions of the material can be studied.

Acknowledgements

The authors gratefully acknowledge Walter Lauriks and Goran Pavic for their valuable comments on the manuscript of this document.

References

[1] A.D. Nashif, D.I.G. Jones, J.P. Henderson, *Vibration Damping*, Wiley-Interscience, 1985.
[2] ASTM-E756-98, *Standard Test Method for Measuring Vibration-damping Properties of Materials*, American society for testing and materials, 1998.
[3] J.-L. Wojtowicki, L. Jaouen, R. Panneton, A new approach for the measurement of damping properties of materials using the Oberst beam, *Review of scientific instruments* 75 (8) (2004) 2569–2574.
[4] Y. Liao, V. Wells, Estimation of complex Young's modulus of non stiff materials using a modified Oberst beam technique, *Journal of Sound and Vibrations* 316 (2008) 87–100.

[5] L. Jaouen, B. Brouard, N. Atalla, C. Langlois, A simplified numerical model for a plate backed by thin foam layer in the low frequency range, *Journal of Sound and Vibrations* 280 (2005) 681–698.
[6] J.-F. Allard, B. Brouard, N. Atalla, S. Ghinet, Excitation of soft porous frame resonances and evaluation of rigidity coefficients, *Journal of the Acoustical Society of America* 121 (2007) 78–84.
[7] J.-F. Allard, M. Henry, L. Boecks, P. Leclaire, W. Lauriks, Acoustical measurement of the shear modulus for thin porous layer, *Journal of the Acoustical Society of America* 117 (4) (2005) 1737–1743.
[8] N. Geebelen, L. Boeckx, G. Vermeir, W. Lauriks, J.-F. Allard, O. Dazel, Measurement of the rigidity coefficients of a Melamine foam, *Acta Acustica United with Acustica* 93 (5) (2007) 783–788.
[9] L. Jaouen, A. Renault, M. Deverge, Elastic and damping characterisations of acoustical porous materials: available experimental methods and applications to a melamine foam, *Applied Acoustics* 69 (12) (2008) 1129–1140.
[10] O. Danilov, F. Sgard, X. Olny, On the limit of an in vacuum model to determine mechanical parameters of isotropic poroelastic materials, *Journal of Sound and Vibrations* 276 (3–5) (2004) 729–754.
[11] S. Ghinet, N. Atalla, Wave approach modeling of sandwich and laminate composite structures with viscoelastic layers, *19th International Congress on Acoustics - ICA07 MADRID*, Spain, 2–7 September, 2007.
[12] S. Ghinet, N. Atalla, Noise transmission loss of orthotropic sandwich composite panels, *Noise-Con 2008*, Dearborn, Michigan, July 28–30, 2008.
[13] A. Renault, Caractérisation mécanique dynamique de matériaux poro-visco élastiques (Dynamic Characterization of Poro-viscoelastic Materials), PhD Thesis, INSA Lyon-Université de Sherbrooke, Qc, Canada, 2008.
[14] B. Hakansson, P. Carlsson, Bias errors in mechanical impedance data obtained with impedance head, *Journal of Sound and Vibrations* 113 (1) (1987) 173–183.
[15] W. Ziolkowski, A. Sliwinski, The influence of the transmission function of the impedance head on the measurement of the complex elastic modulus of a viscoelastic beam by the driving point impedance method, *Journal of Sound and Vibrations* 80 (2) (1981) 209–222.
[16] O. Beslin, J. Nicolas, A hierarchical functions set for predicting very high order plate bending modes with any boundary conditions, *Journal of Sound and Vibrations* 202 (5) (1997) 633–655.
[17] C. Langlois, R. Panneton, N. Atalla, Polynomial relations for quasi-static mechanical characterization of isotropic poroelastic materials, *Journal of the Acoustical Society of America* 110 (6) (2001) 3032–3040.
[18] T. Pritz, Transfer function method for investigating the complex modulus of acoustic materials: spring-like specimen, *Journal of Sound and Vibrations* 72 (3) (1980) 317–341.
[19] L. Jaouen, Contribution à la caractérisation mécanique de matériaux poro-visco-élastiques en vibro-acoustique (Contribution to Poro-viscoelastic Mechanical Characterization in Vibro-acoustics), PhD Thesis, Université du Maine (France)-Université de Sherbrooke, Qc, Canada, 2003.